

Discrete Element Modeling of Railroad Ballast Settlement

Erol Tutumluer
Associate Professor
Phone: (217) 333-8637
Fax: (217) 333-1924
E-mail: tutumlue@uiuc.edu

Hai Huang
Graduate Research Assistant
Phone: (217) 244-6064
E-mail: hhuang14@uiuc.edu

Youssef Hashash
Associate Professor
Phone: (217) 333-6986
E-mail: hashash@uiuc.edu

Jamshid Ghaboussi
Professor Emeritus
Phone: (217) 333-6939
E-mail: jghabous@uiuc.edu

Civil and Environmental Engineering Department
University of Illinois at Urbana Champaign
Newmark Civil Engineering Laboratory
205 North Mathews Avenue
Urbana, Illinois 61801

Draft Manuscript Submitted for the
AREMA 2007 Annual Conference

ABSTRACT

This paper presents findings of a railroad ballast Discrete Element Modeling (DEM) research study focused on investigating ballast settlement under repeated wheel loading. In this approach, the ballast layer is modeled as an assembly of aggregate particles, AREMA No. 24 ballast gradation with different shapes and angularities and rough surface textures. The study matrix considered three different wheel load magnitudes applied on a crosstie at three different load frequencies. Varying load frequencies helped account for different load pulse durations realized under different trafficking speeds. For each DEM solution, the load was applied for up to 100 cycles and the plastic deformations were recorded to indicate resulting ballast settlement. As expected, greater load magnitudes produced larger plastic deformations at one loading frequency. Yet, at a constant applied load magnitude, lower loading frequencies often yielded higher plastic deformations. DEM simulations also conducted with two other aggregate shapes indicated similar impacts of the frequency on ballast settlement.

Key Words: Discrete Element Modeling, Ballast, Aggregate Shape, Repeated Wheel Loading, Settlement, Trafficking Speed

INTRODUCTION

Ballast settlement usually leads to rough track and uneven ride caused by excessive dynamic loading and other track substructure problems. Proper selection of ballast aggregate type, gradation, angularity, and surface texture properties and proper construction and compaction in the field primarily influence ballast layer recoverable

(elastic) and permanent (inelastic) deformation trends under repeated train loading. Recent laboratory and field research studies have shown that frequency of loading or load pulse duration as a result of trafficking speed might also have a significant impact on the increased rate of settlement unbound aggregate layers [1]. A better understanding of the deformation behavior of ballast aggregates to dynamic wheel loading at different frequencies or train speeds will no doubt improve ballasted track designs.

This paper will present results from a Discrete Element Modeling (DEM) research study focused on investigating ballast settlement under repeated wheel loading. In this approach, the ballast layer is modeled as an assembly of aggregate particles, AREMA No. 24 ballast gradation with different shapes and angularities and rough surface textures. The study matrix considered effects of three different wheel load magnitudes applied on a crosstie at three load frequencies studied for three aggregate shape and angularity properties to investigate ballast permanent deformation trends. Important research findings will be presented together with the advantages of this powerful DEM simulation approach as a potential tool for better understanding of the deteriorating railroad infrastructure and scheduling of maintenance and rehabilitation activities.

AGGREGATE IMAGING AIDED DISCRETE ELEMENT MODELING

An innovative Discrete Element Modeling (DEM) approach was recently adopted and implemented with established aggregate shape libraries ranging from flat and elongated to cubical and angular to round [2]. The principle of DEM for studying assemblies of granular particles interacting with each other through contact laws in incremental time domain and the essential features of the implemented imaging aided DEM approach were

explained in detail in the 2006 AREMA Conference paper published by the authors [2]. The approach simply uses ballast aggregate shape, angularity and surface texture properties as indices quantified from digital image equipment to define an individual aggregate particle as a 3-dimensional block element for input in the DEM program called DBLOKS3D [3]. Using the indices defined as Flat and Elongated (F&E) ratio, Angularity Index (AI), and Surface Texture (ST), this imaging aided DEM approach can quantify individual effects resulted by any single factor such as angularity, surface texture, and flatness and elongation of the aggregate material primarily used in the ballast layer for strength and deformation properties. Figure 1 shows available representative aggregate shapes, i.e., library of aggregate shapes used as individual block elements in DEM, as listed in terms of morphological properties.

BALLAST LAYER PREPARATION

AREMA specification requires ballast aggregate to be cubical with crushed faces which correspond to shape 1 in Figure 1. It is believed to be the best aggregate, such as crushed stone, with high strength, superior load distribution and ballast performance. Aggregate shapes 3 and 4 are sub-rounded and rounded particles which often correspond to crushed or uncrushed gravel type of aggregate. Shape 8 in Figure 1 represents a flat and elongated type of aggregate particle which is less favorable in railroad engineering practice since it is low load bearing and due to its tendency to more easily break and degrade. To compare ballast deformation trends for different aggregate shape properties, shapes 1, 3, 8 were chosen in this study as the representative aggregate sources to construct and subject the ballast layer in DEM simulations to repeated loading.

AREMA No. 24 ballast gradation was used for all ballast aggregate samples with different shapes. Aggregate surface texture, roughness or smoothness related to microtexture, was also kept the same to consider only rough textured samples in this study. Another assumption made was that ballast aggregates were non-breakable and no abrasion was tolerated to ensure that all ballast samples were of the same solid shape throughout the DEM simulation process. This way, any difference in simulation results between different ballast samples would be only attributable to the aggregate shape.

The ballast box test proposed by Norman [4] was originally used for ballast field strength and settlement testing purposes in the laboratory [5]. Accordingly, the ballast box dimensions were selected for a single tie-ballast effective contact area. In this study, the length of the ballast simulation domain was set to be the same as the length of the ballast ox which was equal to the tie spacing. Figure 2 shows the plan view of the simulation setup with the half tie length and a corresponding ballast width of 0.61 m assigned instead of 0.3 m used in ballast box test by Norman [4]. This way, the simulation adequately considered the ballast shoulder movement.

Ballast samples were constructed by dropping layers of aggregate sized according to the AREMA No. 24 gradation without compaction. Figure 3 shows the ballast layer, which consisted of 3,136 aggregate particles from shape library 1 (see Figure 1).

LOADING MAGNITUDE AND FREQUENCY

Dynamic loading on the top of a tie is determined by un-sprung excitation and train speed. Assuming that there is no excitation coming from the train itself and the track is perfectly smooth; the load magnitude and duration (or frequency) on the top of the tie is

determined by the train weight and speed. They are derived from a basic semi-coupled dynamic track model where the track is treated as a beam on continuously elastic support, which is expressed as follows according to Esveld [6]:

$$EI \frac{d^4 y}{dx^4} + \rho \frac{d^2 y}{dt^2} + c \frac{dy}{dt} + ky = P \delta(x - vt) \quad (1)$$

where: EI = rigidity of the rail;

y = vertical displacement of the rail;

x = longitudinal coordinate;

t = time;

ρ = unit weight of the rail;

c = damping of the substructure;

k = unit length track substructure stiffness;

P = train weight;

v = train speed, and;

δ = Delta function describing the position of the load.

Load magnitude and duration underneath the rail, i.e., on top of the tie, can be obtained from rail deformation-time relationship derived in Equation 1 for different train speeds [6]. Accordingly, Figure 4 shows the loading profile on top of a tie representing a 160,000-kg train car moving at a speed of 28 km/h. Since the load pulse shown in Figure 4 is of a half-sine wave shape with the second half portion considered for 0.5-second rest period, it is considered as a 1 Hz load pulse in this study.

SIMULATION TEST MATRIX

After the half ballast section simulation was developed, a half tie was generated and placed on top of the ballast layer followed by the applications of individual dynamic loading profiles derived from Equation 1 and the load pulse shapes shown in Figure 4. Different combinations of DEM simulations were performed to consider a total of three load magnitudes, three load frequencies (1 Hz, 5 Hz, and 10 Hz corresponding to train speeds of 28, 140, and 280 km/h, respectively), and three ballast aggregate shapes, i.e., libraries 1, 3, and 8. Table 1 lists in detail the variables and the DEM simulation test matrix studied.

SIMULATION RESULTS AND ANALYSES

Ballast settlement, i.e., permanent deformation or rut depth, was recorded with the number of load cycles for all the DEM simulations listed in Table 1. Each repeated loading test was performed up to 100 cycles but not up to commonly tested three log cycles due to intense computational needs of DEM simulations. In this paper, only results of repeated loading simulations that considered 120-kN normal loading are presented. For the ballast layer with cubical and angular shaped aggregates (shape library 1), Figure 5 shows settlement under the moving train load graphed with load cycles investigated at all three train speeds (frequencies). It can be clearly seen that train speed has a significant impact on ballast settlement as obtained from these DEM simulations. The faster the train goes (higher loading frequency or shorter pulse durations) the higher are the permanent deformations accumulated under the same load magnitude for the same

ballast aggregate material. Kim and Tutumluer [1] reported similar findings on unbound aggregate permanent deformation trends from both laboratory repeated load triaxial testing of compacted aggregate specimens and full-scale field testing of thick airport granular layers. It is indeed encouraging to see similar trends obtained here from the DEM simulations.

Figure 6 indicates for the library 1 aggregate shape permanent deformations produced by a static loading and the same magnitude dynamic loads applied at different frequencies. It can be observed that the settlement produced by the static load is lower than the permanent deformation due the 1-Hz dynamic loading. As the loading frequency increases, the settlement is estimated to peak at a frequency between 1 and 5-Hz loadings, then, it decreases to a rut accumulation less than the starting value due to the static loading. Therefore, there exists a frequency analogous to a natural frequency, possibly of the track structure simulated here, which could produce the maximum settlement. This kind of a trend in peak permanent deformations was found to exist for the two other aggregate shapes, libraries 3 and 8, also studied.

Figures 7 and 8 show the effects aggregate shape on ballast settlement in comparison to the results presented for the library 1 aggregate shape. In Figure 7, this kind of comparison is made between the performances of the ballast layers with the cubical-angular shaped library 1 aggregate and the elongated and rounded shaped library 8 aggregate. Because the elongated aggregate yields smaller settlement than the cubical one should not imply that the ballast layer with the flat and elongated aggregate particles can outperform the ballast with the cubical-angular library 1 aggregate. Note that in the

DEM simulations the flat and elongated particles were not allowed break although in reality they tend to easily break and degrade under heavy wheel loading.

Figure 8 compares the performances of two cubical ballast aggregate shapes, however, library 1 is angular and library 3 is rounded. Note that the ballast layer with the rounded particles yields much less settlement than the ballast with angular aggregate. This is in general against the common belief and what is normally expected. Angular aggregates have been known to be always better than rounded aggregates in the sense of higher strength properties and improved stability due to better interlock. Nevertheless, when it came to permanent deformation trends, this was not the case from DEM simulations. One may offer two possible explanations in relation to what was simulated in this study. One explanation is that during ballast aggregate particle packing, angular particles will result in larger air voids, e.g., consider uncompacted voids tests performed for determining angularity of fine and coarse aggregate, due to less efficient packing, which gives in the end each aggregate particle more room to move, shakedown and consolidate. Another explanation related to the simulation test setup is that since only one tie is simulated in the train moving direction, the interactions between ties are not considered in the DEM simulations and the ballast aggregate movement along the traffic direction is limited by the transverse plane (see Figure 2) in the middle of the two adjacent ties.

Figure 9 shows the recorded residual forces acting on the transverse vertical plane (see Figure 2) for the library 1 (angular) and library 3 (rounded) aggregate shapes. The ballast layer with the rounded aggregates has larger residual force on the middle plane than the force created by the angular aggregate. It suggests that, lateral confinement in

the test setup for the rounded aggregate particles is higher than the angular one, which would definitely help reduce the permanent deformation tendency of the library 3 rounded aggregate particles.

CONCLUSIONS

In this paper, an innovative aggregate imaging aided Discrete Element Modeling (DEM) approach was used to study ballast settlement under moving train loading. Load frequencies or load pulse durations governing the various train speeds and ballast aggregate shape properties, cubical versus elongation and angular versus rounded aggregates, were the two main factors studied in the context of settlement or permanent deformation accumulation trends. From the DEM simulations for up to 100 repeated load applications, it was found that reducing the train speed, such as in the slow orders, (or decreasing the applied loading frequency by increasing the load pulse durations) often results in a significant increase in the rut accumulation. However, static loading induced smaller permanent deformations than the 1-Hz loading. Therefore, a critical loading frequency to give maximum rutting was found to be between 1 and 5 Hz loadings.

Effects of ballast aggregate shape was also found to influence ballast settlement. The DEM simulations that considered single tie tests resulted in lower ballast settlements for rounded aggregate particles possible due to lesser tendency to shakedown and consolidate. For future ballast settlement simulations, it will be worthwhile to consider a modified ballast box for the half tie and half ballast width railroad track geometry with at least three ties included to model longitudinal confinement and movement of ballast aggregate. Future work should also include effects of different ballast gradations.

ACKNOWLEDGEMENTS

The authors would like to thank the Association of American Railroads (AAR) for their financial support of this research study through the AAR Affiliated Research Laboratory established at the University of Illinois at Urbana-Champaign.

REFERENCES

1. Kim, I.T. and Tutumluer, E., "Field Validation of Airport Pavement Granular Layer Rutting Predictions," In Transportation Research Record 1952, Journal of the Transportation Research Board, National Research Council, Washington, D.C., 2006, pp. 48-57.
2. Tutumluer, E., Huang, H., Hashash, Y., and Ghaboussi, J., "Aggregate Shape Effects on Ballast Tamping and Railroad Track Lateral Stability," AREMA Annual Conference, 2006.
3. Nezami, E. G., Zhao, D., Hashash, Y., and Ghaboussi, J., "A Fast Contact Detection Algorithm for 3-D Discrete Element Method," Computers and Geotechnics, Vol. 31, 2004, pp. 575-587.
4. Norman, G., "Ballast Box Experiments for Evaluating Ballast Field Performance," FRA report 82-291 P, 1982.
5. Stewart, H.E., Selig, E.T., and Norman, G.M., "Failure Criteria and Lateral Stresses in Track Foundations," Transportation Research Record, 1022, pp 59-64, 1985.

6. Esveld, C., "Modern Railway Track," Second Edition, MRT-Productions, the Netherland, 2001.

LIST OF TABLES

Table 1. The DEM Simulation Test Matrix

LIST OF FIGURES

Figure 1. Imaging Aided Discrete Element Aggregate Particle Shapes [2]

Figure 2. Plan View of Ballast Settlement DEM Simulation

Figure 3. Ballast Sample of a Half Railroad Section with Angular and
Cubical Aggregates of Shape Library 1

Figure 4. Single Tie Load Pulse of a 160-Mg Car Applying Loading at 1-Hz Frequency

Figure 5. Permanent Settlement of Ballast with Aggregate Shape Library 1 (Cubical –
Angular) at Three Different Loading Frequencies

Figure 6. Permanent Deformations Produced by the Static Load and the Same
Magnitude Dynamic Loads Applied at Different Frequencies

Figure 7 Comparisons of Ballast Settlement between Aggregate Shape Library 1 (Cubical
– Angular) and Shape Library 8 (Elongated – Rounded) at Three Loading Frequencies

Figure 8. Comparisons Ballast Settlement between Aggregate Shape Library 1 (Cubical –
Angular) and Shape Library 3 (Cubical – Rounded) at Three Loading Frequencies

Figure 9. Residual Forces Crated on the Transverse Vertical Plane
(The Middle Plane between Two Ties)

Table 1. The DEM Simulation Test Matrix

Load Magnitude (kN)	Frequency (Hz) (Train Speed, km/h) *	Shape Library 1 (Cubical - Angular)	Shape Library 3 (Cubical - Rounded)	Shape Library 8 (Elongated - Rounded)
90	1 (28)	X		X
	5 (140)	X		X
	10 (280)	X		X
120	1 (28)	X	X	X
	5 (140)	X	X	X
	10 (280)	X	X	X
150	1(28)	X		X
	5 (140)	X		X
	10 (280)	X		X

* According to Equation 1 and Esveld [6]

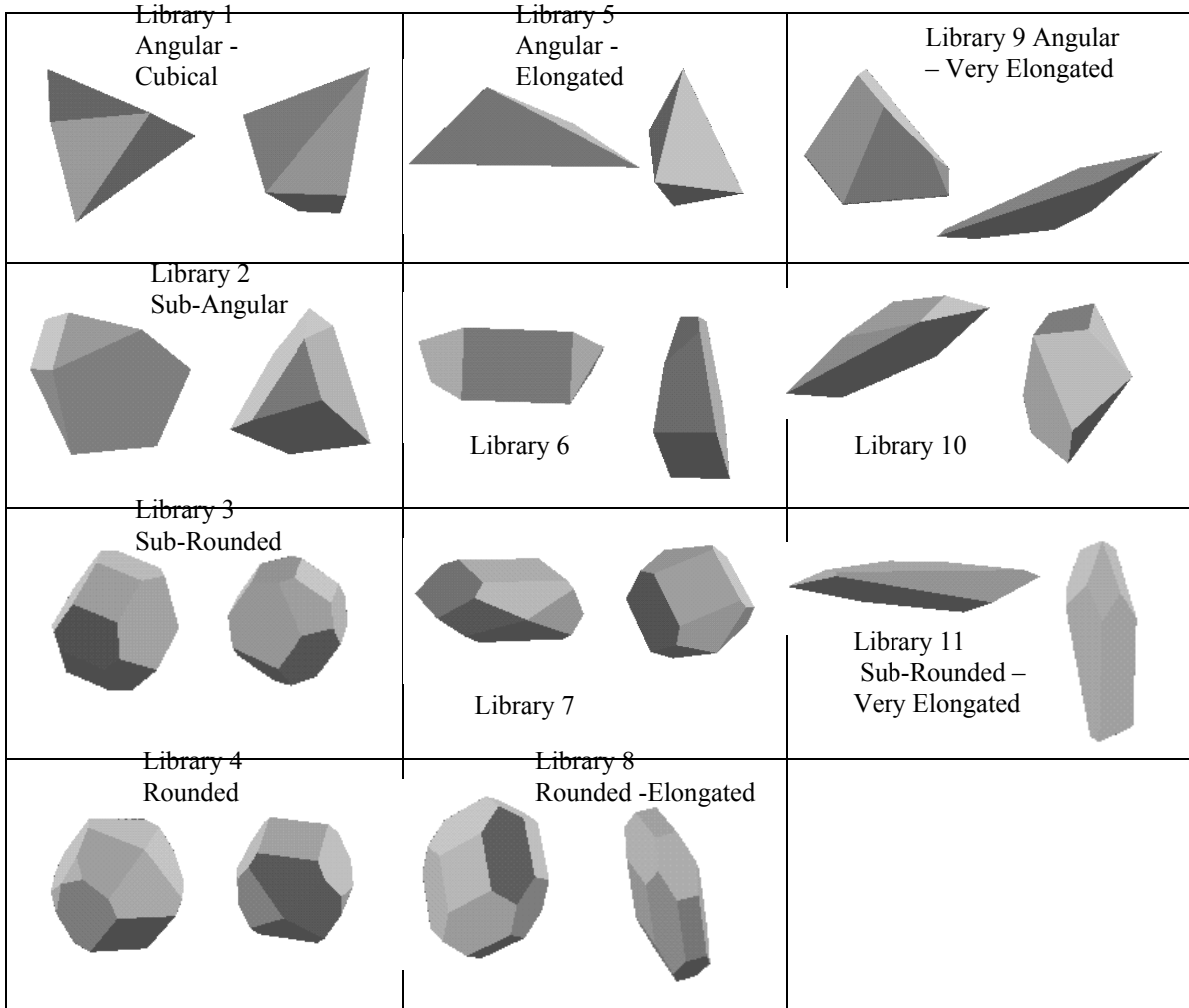


Figure 1. Imaging Aided Discrete Element Aggregate Particle Shapes [2]

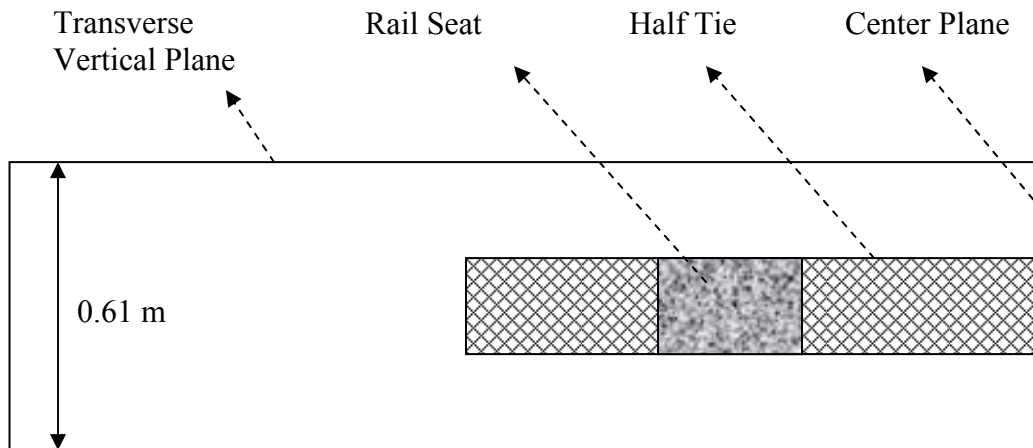


Figure 2. Plan View of Ballast Settlement DEM Simulation



Figure 3. Ballast Sample of a Half Railroad Section with Angular and Cubical Aggregates of Shape Library 1

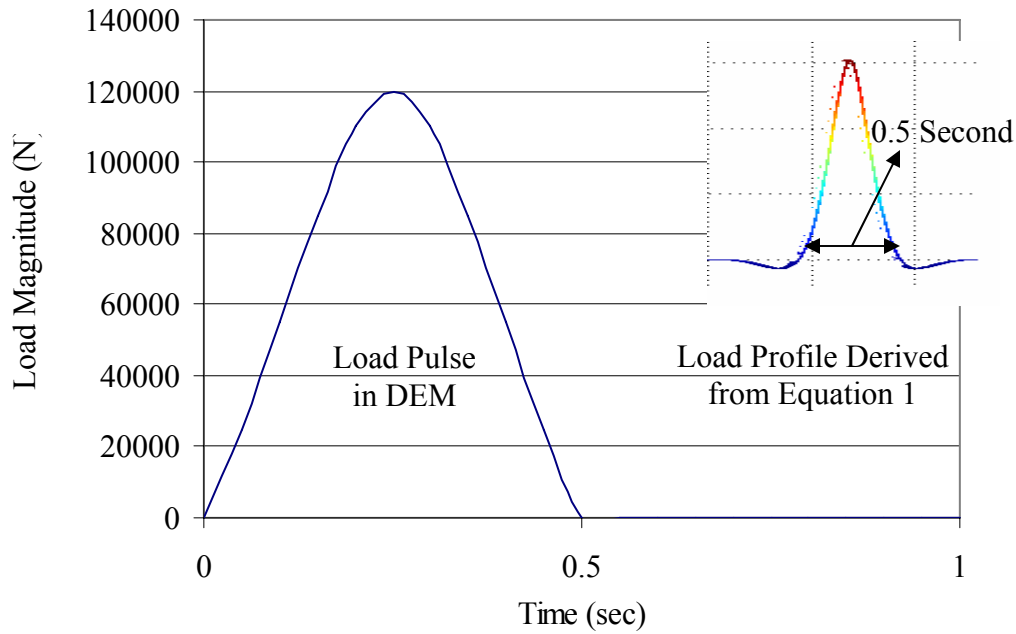


Figure 4. Single Tie Load Pulse of a 160-Mg Car Applying Loading at 1-Hz Frequency

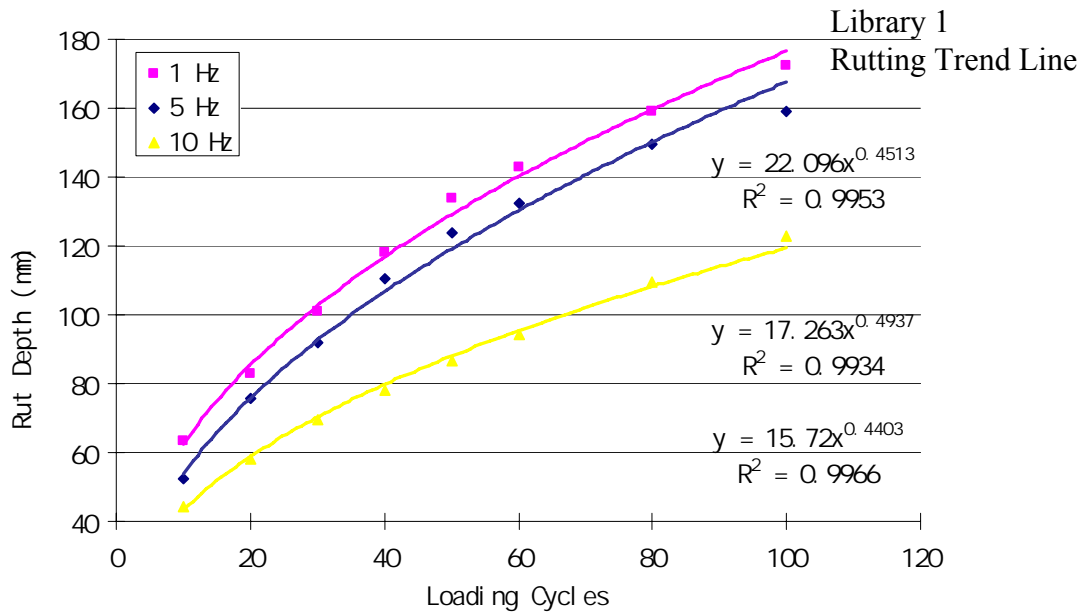


Figure 5. Permanent Settlement of Ballast with Aggregate Shape Library 1 (Cubical – Angular) at Three Different Loading Frequencies

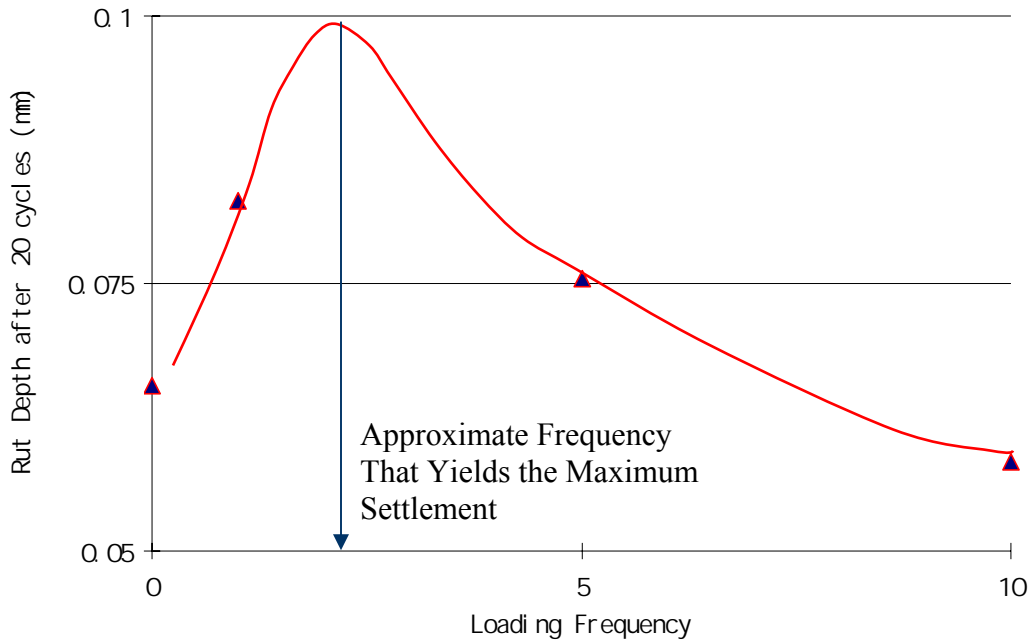


Figure 6. Permanent Deformations Produced by the Static Load and the Same Magnitude Dynamic Loads Applied at Different Frequencies

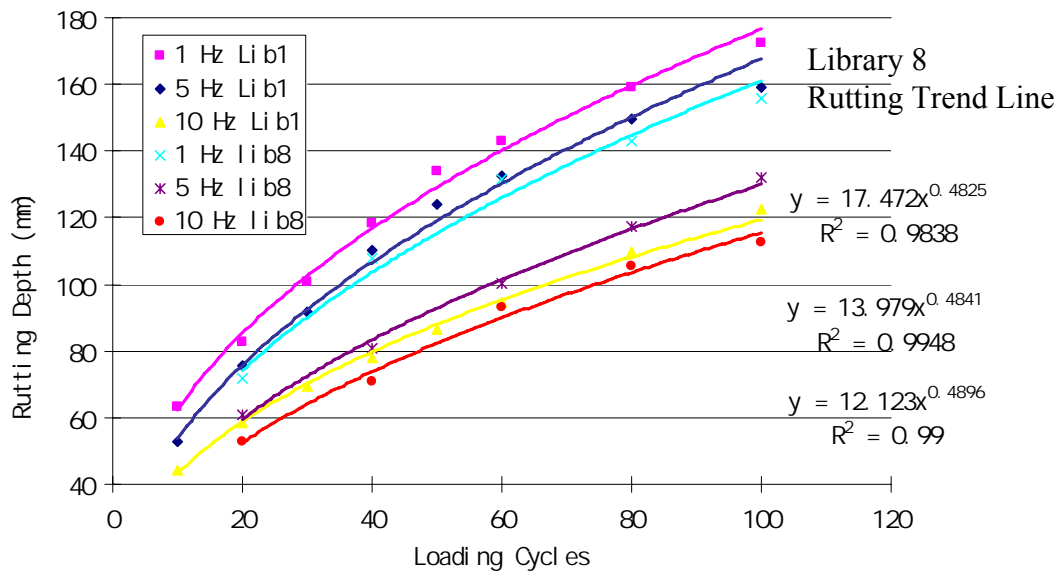


Figure 7 Comparisons of Ballast Settlement between Aggregate Shape Library 1 (Cubical - Angular) and Shape Library 8 (Elongated - Rounded) at Three Loading Frequencies

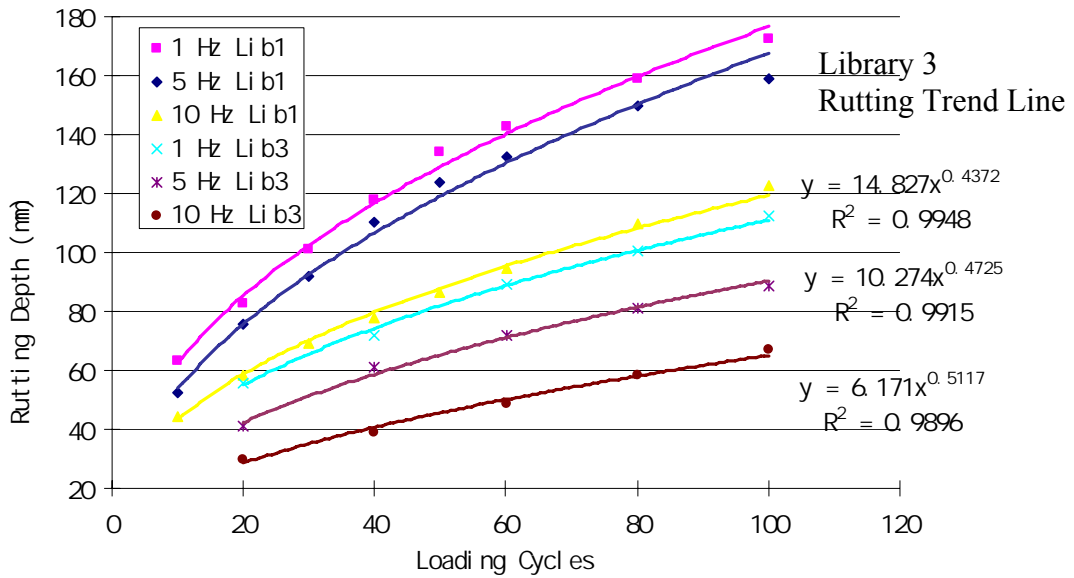


Figure 8. Comparisons Ballast Settlement between Aggregate Shape Library 1 (Cubical Angular) and Shape Library 3 (Cubical – Rounded) at Three Loading Frequencies

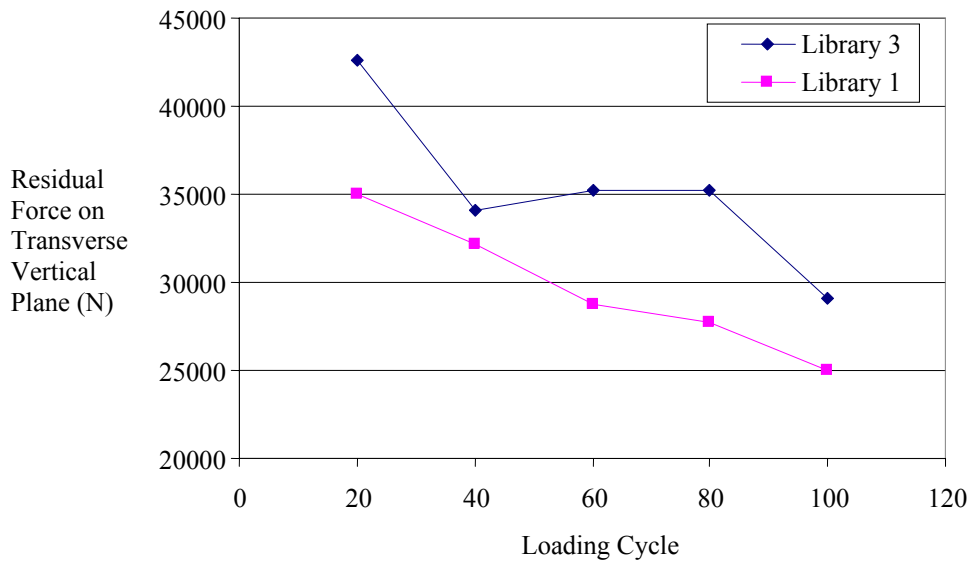


Figure 9. Residual Forces Crated on the Transverse Vertical Plane (The Middle Plane between Two Ties)